JOURNAL OF MATERIALS SCIENCE 37 (2002) 955–961

The production of Al-Mg alloy/SiC metal matrix composites by pressureless infiltration

A. ZULFIA*, R. J. HAND
Department of Engineering Materials, The University of Sheffield, Sir Robert Hadfield Building, Mappin Street, Sheffield, S1 3JD, UK
E-mail: r.hand@sheffield.ac.uk

Metal matrix composites have been produced by pressureless infiltration of Al-Mg alloys into SiC preforms at 900°C under N_2 for different infiltration times. The wettability of the ceramic reinforcement by the Al-Mg alloy is crucial in determining whether an MMC can be produced by pressureless infiltration. Sessile drop results show that Al alloys with Mg contents greater than 8 wt% had a contact angle lower than 90°C after 5 minutes contact time. This was in agreement with the pressureless infiltration results as MMCs have been produced after 30 minutes with these alloys. Sessile drop experiments also show that SiC is similarly wetted by Al-Mg alloys under both N_2 and Ar. It is concluded that the infiltration process does not involve the intermediate nitride phase suggested by other authors.

1. Introduction

Metal matrix composites (MMCs) reinforced with ceramic reinforcements offer high strength and modulus, as well as good high-temperature properties, when compared with corresponding monolithic alloys and are promising materials for automotive and aerospace applications. MMC production via liquid metal infiltration has the potential to be an economic process. The non-wetting nature of many ceramics by molten aluminium, however, which results in poor ceramic-metal interfaces and incomplete infiltration, is an obstacle. Attempts to overcome this have usually involved the use of pressure or vacuum to assist the infiltration process [1, 2]. However, a more recent development in the production of aluminium matrix MMCs has been a pressureless infiltration process. The process involves the infiltration of a liquid Al-Mg alloy into a porous preform under N_2 at atmospheric pressure, which means that the process can be carried out using simpler equipment than that required for vacuum or pressure assisted infiltration [3, 4]. This infiltration process is related to the Lanxide or directed melt oxidation process for ceramic matrix composite production and has, in fact, been patented under the Primex^{TM} name by the Lanxide Corporation.

The relationship between infiltration pressure and wetting has been reported by Mortensen and Cornie [5]. For non-wetting systems they report that the pressure necessary for infiltration becomes infinitely large as the contact angle between touching reinforcements approaches 0. This necessitates the formation of voids in regions of filler (preform) contact. They argue that infiltration into these regions is actually preferred since the metal will be drawn into regions where the filler surface area to metal volume ratio is high. However, the non-wetting nature of many ceramics by molten metals results in flocculation, voids at interfaces, and incomplete infiltration and hence the requirement is for high infiltration pressures [6].

Yang and Xi [7] have shown that pressureless infiltration of porous media requires a wetting or contact angle lower than 90°, regardless of the dynamic or kinetic effects and it is believed that both the presence of Mg as a dopant and an N_2 atmosphere are essential to improve the wettability of SiC by Al thus allowing pressureless infiltration to proceed [8]. Schiroky *et al*. [9] claimed that when a ceramic preform is in intimate contact with the molten Al-Mg alloy, Mg evaporates and diffuses into the preform. There, Mg reacts with the nitrogen atmosphere to form a coating of magnesium nitride (Mg_3N_2) on the ceramic reinforcement. When molten aluminium comes into contact with Mg_3N_2, it is reduced to form AlN, with Mg dissolving into and re-evaporating from the alloy:

$$Mg_3N_2 + 2Al \rightarrow 2AlN + 3Mg. \quad (1)$$

It is claimed that this reaction induces wetting and thus allows for the pressureless infiltration of aluminium alloys into ceramic preforms. However although the wettability of SiC by Al has been investigated by a variety of authors [10–13] little attention has been paid to the effect of atmosphere on the wettability of SiC by Al-Mg alloys. Therefore in this paper we examine the infiltration of SiC preforms by a number of Al-Mg

Present Address: Department of Metallurgy, The University of Indonesia, Kampus Baru UI, Depok 16424, Indonesia.

alloys and relate the results to sessile drop measurements of the contact angle between these alloys and SiC.

2. Experimental procedure

Alloy samples, approx. 30 × 15 × 10 mm in size were cut from in-house prepared, cast Al-Mg alloy blocks (see Table I). The alloys were prepared by induction melting from commercial purity Al and Mg. After cutting the blocks were ground on emery paper and washed in deionised water. The prepared block was placed on the top of a loose bed of SiC particles with a mean particle size of 63 μm (Sigma Aldrich). This preform contained 50 Vf% SiC based on the Al block (see Fig. 1). The prepared sample was placed into a vertical tube furnace, which was then flushed overnight with nitrogen gas (nominally oxygen free; 99.99% pure) before heating. The samples were heated under the same nominally oxygen free nitrogen and to prevent unwanted gases from entering the furnace chamber, all experiments were conducted under a slight positive pressure of nitrogen; this was achieved by bubbling the exit gas. The furnace was ramped at 200°C/hour to a soaking temperature of 900°C. The soaking temperature was maintained for 30 mins, 1, 2, 4, 8 hours. The sample was furnace cooled.

To investigate the contact angle between Al and SiC, sessile drop experiments were carried out primarily under N_2. Some experiments were also conducted under Ar. 1-2 g mass of the alloy as used in pressureless infiltration, i.e, commercial purity Al, Al-2Mg, Al-5Mg, Al-8Mg, Al-10Mg, and Al-14Mg alloys were cut from the ingots. The alloy pieces were ground to an approximately cubic shape then immediately immersed in dry methanol. The samples were then ultrasonically cleaned. Sintered α-silicon carbide (SSiC) (Hexoloy) was used as a substrate. The α-SSiC was slit with a diamond saw to produce pieces approximately 10 × 10 × 5 mm. These samples were ground and polished on one flat. As shown in Fig. 2, the α-SSiC was placed on an alumina boat with the polished surface upward, the rest of alumina boat being filled with titanium sponge to act as a getter for residual oxygen in the nitrogen atmosphere. The prepared sample was placed in a sealed furnace chamber with a viewing port through which a camera could be focussed on the sessile drop. The apparatus was evacuated for 4 hours and then either an N_2 or Ar atmosphere was introduced before the sample was heated to 900°C. After reaching temperature the drop was photographed at 5 minute intervals for 1 hour.

TABLE I Chemical analysis of parent metals and alloys used for pressureless infiltration, (ICP)

Element	Al-2Mg	Al-5Mg	Al-8Mg	Al-10Mg	Al-14Mg
Cu	<0.02%	<0.02%	<0.02%	0.02%	<0.02%
Zn	<0.02%	<0.02%	<0.02%	<0.02%	<0.02%
Fe	0.05 ± 0.02%	0.05 ± 0.02%	<0.02%	0.04 ± 0.02%	0.02%
Mn	<0.02%	<0.02%	<0.02%	<0.02%	–
Ni	<0.02%	<0.02%	<0.02%	<0.02%	<0.02%
Ti	<0.02%	<0.02%	<0.02%	<0.02%	<0.02%
Cr	<0.02%	<0.02%	<0.02%	<0.02%	<0.02%
Mg	2.18 ± 0.02%	4.79 ± 0.04%	8.32 ± 0.08%	9.74 ± 0.08%	14.0 ± 0.1%
Si	<0.02%	<0.02%	<0.02%	0.02%	0.05 ± 0.02%
Na	<0.005%	<0.005%	<0.005%	<0.005%	<0.001%

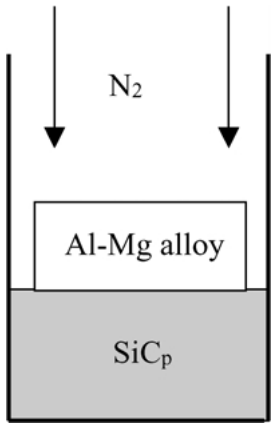

Figure 1 Schematic diagram of the arrangement employed in pressureless infiltration experiment.

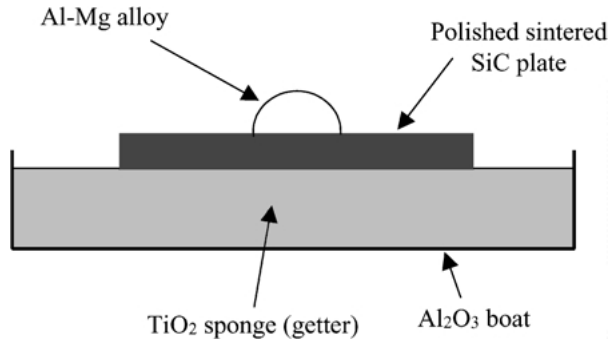

Figure 2 Schematic diagram of the sessile drop experiment.

The microstructures of the MMCs produced by the pressureless infiltration were characterised using optical and scanning electron microscopy (CAMSCAN SEM) coupled with energy dispersive spectroscopy (EDS; Link Analytical). Additional phase identification was carried out using X-ray diffractometry (XRD; Philips 1710 Diffractometer). The hardness of the product was measured from the top to the bottom of the infiltrated section using a Vickers hardness indenter with a 20 kg load. For this load the indent size was usually between 300–650 μm; the largest microstructural features for the SiC reinforced materials are typically 60–100 μm. Each hardness quoted is the average of 3 measurements. The volume fraction of porosity within the product was measured by means of image analysis using an optical microscope in conjunction with a computer running image analysis software (PC-Image 2.2). The sample used for this study was the same as that used for the metallograpy investigations. The porosity measurements were made at 2 different magnifications i.e, 500X and 100X. Between 20 and 25 randomly selected regions of each mounted and polished sample were measured. It was checked that the same result was obtained at both scales of size. Thus, the volume fraction of porosity could be determined directly, and

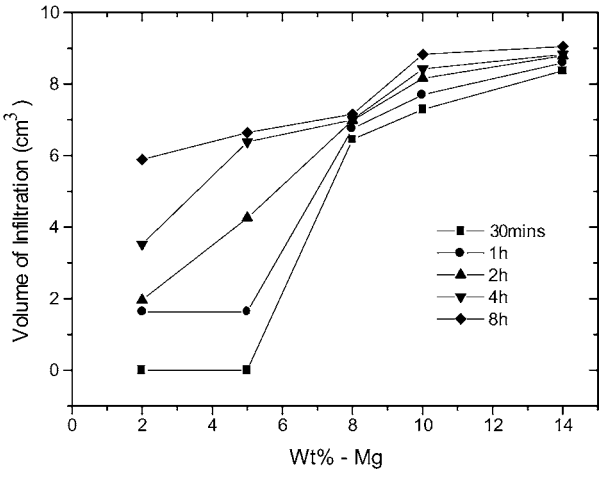

Figure 3 Volume of infiltration as a function of Mg content for infiltration of SiC by Al-Mg alloys at 900°C, under N_2 atmosphere.

the results from these regions were averaged. The field area for each measurement was 260100 pixels.

3. Results

The results of pressureless infiltration of Al-Mg alloys into loose bed SiC preforms are summarized in Fig. 3 which shows the variation of infiltration volume, calculated from the cross-sectional area of the crucible (cylinder) multiplied by the distance that the molten Al had penetrated into the preform. It is clear that no infiltration occurs for low Mg contents at short times. At higher Mg contents, there is little variation in the degree of infiltration with time for the times tested. For low Mg contents there was a more significant dependence of the degree on infiltration on time for the range of times tested.

The microstructures of the products are shown in Fig. 4. In general the microstructures are similar to each other. XRD indicates that all of the products contain Mg_2Si, SiC and Al; example XRD patterns for samples infiltrated with Al-10Mg are shown in Fig. 5. There was also some indication that the product contained Al_2O_3, and Al_4C_3 (see also Fig. 6). A rough estimate of the extent of Al_4C_3 formation has been obtained by simply comparing the intensity of the aluminium carbide and SiC X-ray peaks in the composites. This showed that the amount of Al_4C_3 increased with increasing infiltration time and Mg content (Fig. 7). There was no evidence of nitridation of the aluminium alloy as AlN or Mg_3N_2 could not be detected by XRD, and no nitrogen was detected in EDS.

Fig. 8a shows that the contact angle of Al-8Mg, Al-10Mg and Al-14Mg alloys in nitrogen atmosphere was lower than 90° after 5 minutes contact time while for lower Mg contents the contact angle was still higher than 90° even after 1 hour contact time. Similar results were obtained for these alloys tested under Ar (Fig. 8b).

As found by other authors the hardness and porosity was not uniform within the composites produced by this method [14–16]. The hardness of the composites varied from the top to the bottom of the composites (Fig. 9), and the average hardness increased with increasing of Mg content in Al-alloy and increasing infiltration time. In contrast the porosity decreased with longer infiltration time (Figs 10 and 11).

4. Discussion

The results given here are in accordance with those of other authors which have established that the presence of Mg can allow pressureless infiltration of SiC by Al. As mentioned above it has also been suggested that the presence of a nitrogen atmosphere is essential for this process with the formation of an intermediate nitride being a crucial stage in the process. However other authors suggest that Mg weakens the Al_2O_3 barrier present on the Al surfaces by replacing it with spinel which can be penetrated by the molten Al [17–19]. No Mg_3N_2 or AlN was detected in any of the SiC reinforced systems. Thus, either any AlN or Mg_3N_2 formed was present in quantities below the detection limit in XRD, and below the nitrogen detection limit in EDS, or these nitride phases were not formed and infiltration does not proceed via the formation of these phases. It is worthy of note that in magnesium doped directed melt oxidation of Al, Gu and Hand [20] detected, by XRD, AlN, which had formed when an air atmosphere had been depleted of its oxygen. They also detected the nitrogen in the AlN features in their samples by EDS. Thus it seems likely that the failure to detect AlN here by XRD or EDS indicates that the nitride phases are not formed. In addition the sessile drop results indicate that Ar and N_2 have virtually identical effects on the wetting of SiC by Al-Mg alloys.

As no spinel was detected in the reaction products it is not obvious that the infiltration process is dependent on the formation of spinel, although other authors have suggested this mechanism and there is plenty of evidence that directed melt oxidation does proceed in this fashion [21, 22]. Furthermore we have previously reported that the addition of 2 wt% Si to a system doped with 1 wt%-Mg leads to infiltration even though 1 wt%-Mg on its own does not give infiltration [23]. If the formation of magnesium nitride was the initial step responsible for promoting infiltration it seems unlikely that adding 2 wt%-Si to a system that does not infiltrate, namely 1 wt%-MgI would lead to infiltration, given that 2 wt%-Si on its own also does not give infiltration. However if even 1 wt%-Mg leads to some breakdown of the Al_2O_3 layer to spinel giving splits in the oxide layer then the Si could have a sufficient effect on the aluminium to enable wetting. It seems plausible, therefore although not proven, that breakdown of the protective alumina layer by spinel formation does occur during pressureless infiltration.

As noted above Gu and Hand [20] report that AlN can be formed when oxygen is depleted in directed melt oxidation in air. It is believed that the lower temperatures used here (900°C compared with 1150°C) prevent AlN formation. However for successful pressureless infiltration it is clear that oxygen must be excluded to enable the process to proceed without oxidation and thus it would seem probable that the major reason for using a nitrogen atmosphere is to prevent 'poisoning' of the infiltration process by oxide formation.

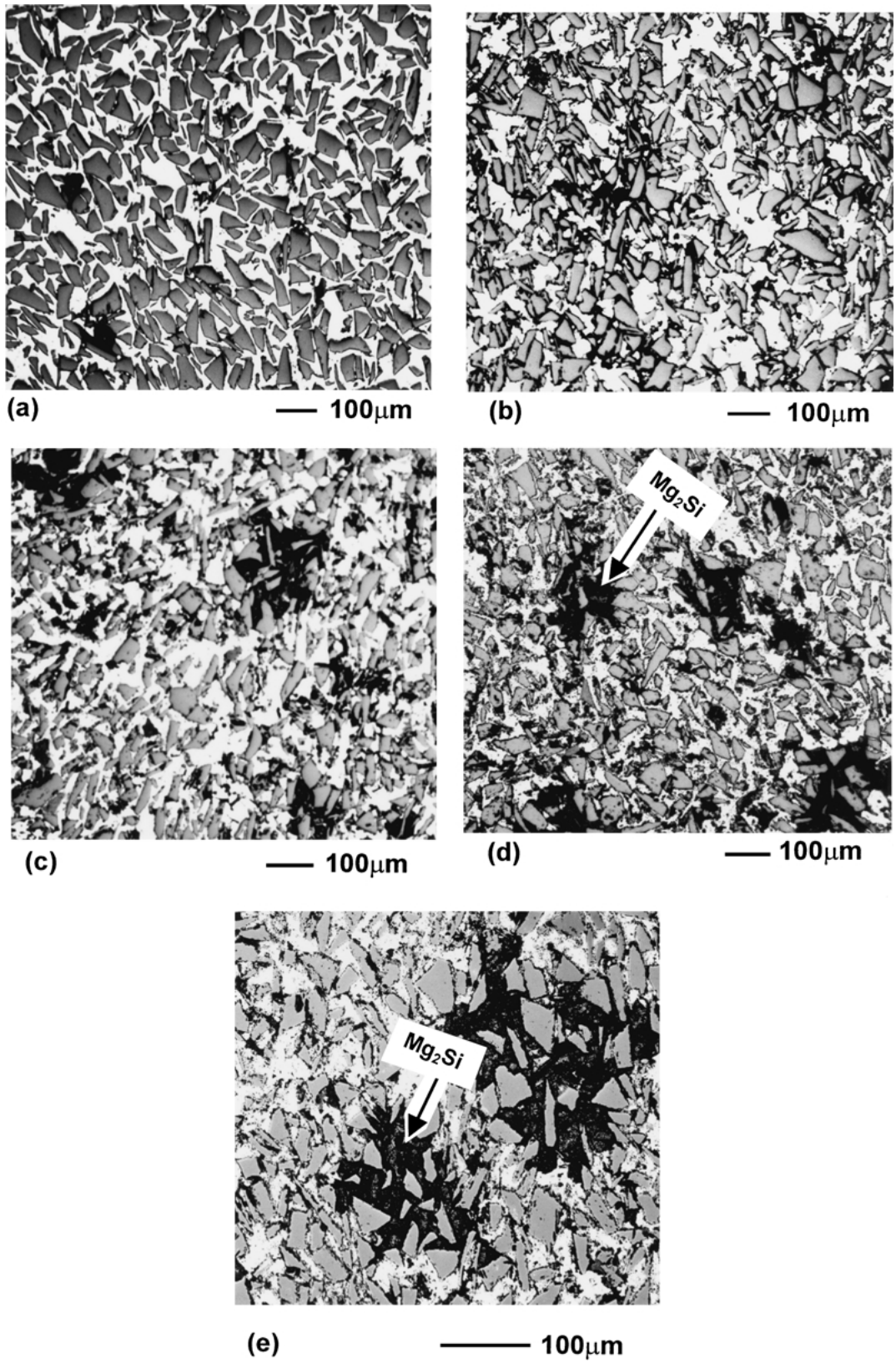

Figure 4 Optical micrographs of SiC infiltrated by Al-Mg alloys after pressureless infiltration at 900°C for 8 hours. (a) 2 Mg, (b) 5 Mg, (c) 8 Mg, (d) 10 Mg and (e) 14 Mg.

The sessile drop experiments demonstrate that the contact angle of aluminium on SiC was reduced with addition of 8 wt%-Mg, 10 wt%-Mg and 14 wt%-Mg at 900°C under N_2 atmosphere (Fig. 8a) as well as increasing the contact time. However with the Al-2Mg and Al-5Mg alloys, the contact angle was greater than 90° even after 1 hour contact time. This suggests that infiltration should not occur after 1 hour with the low Mg content alloys. However limited infiltration was observed in the alloy systems, even after 1 hour, with the infiltration becoming more extensive as time increased (see Fig. 3) which suggests that the contact angle must reduce at longer times.

However there is evidence of Mg_2Si and Al_4C_3 formation in the SiC reinforced system (along with small amounts of Al_2O_3). SiC is thermodynamically unstable

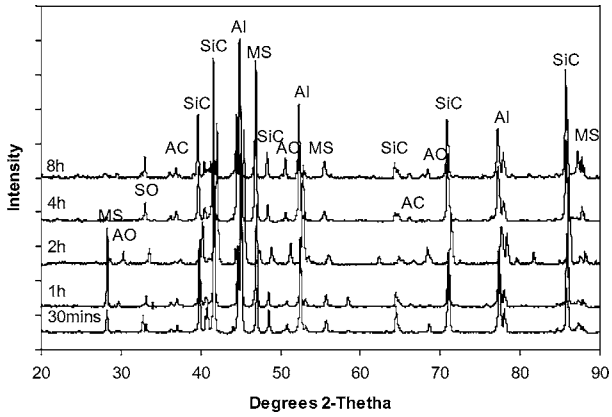

Figure 5 XRD pattern for Al-10Mg alloy/SiC MMC produced by pressureless infiltration at 900°C (Key : MS : Mg_2Si, AC : Al_3C_4, AO : Al_2O_3).

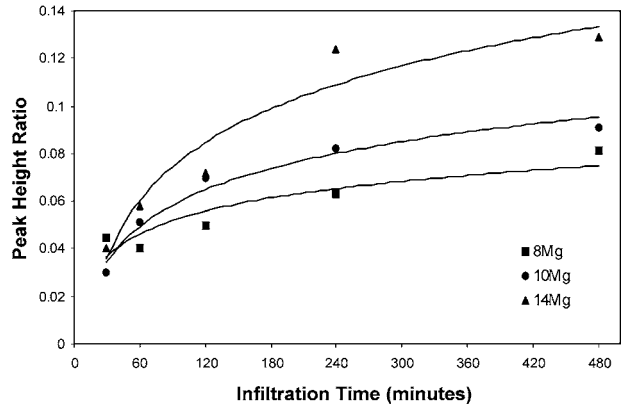

Figure 7 XRD peak ratio of Al_4C_3/SiC interfacial reaction for Al-Mg alloys/SiC MMCs produced by pressureless infiltration process at 900°C for different infiltration times under N_2 atmosphere.

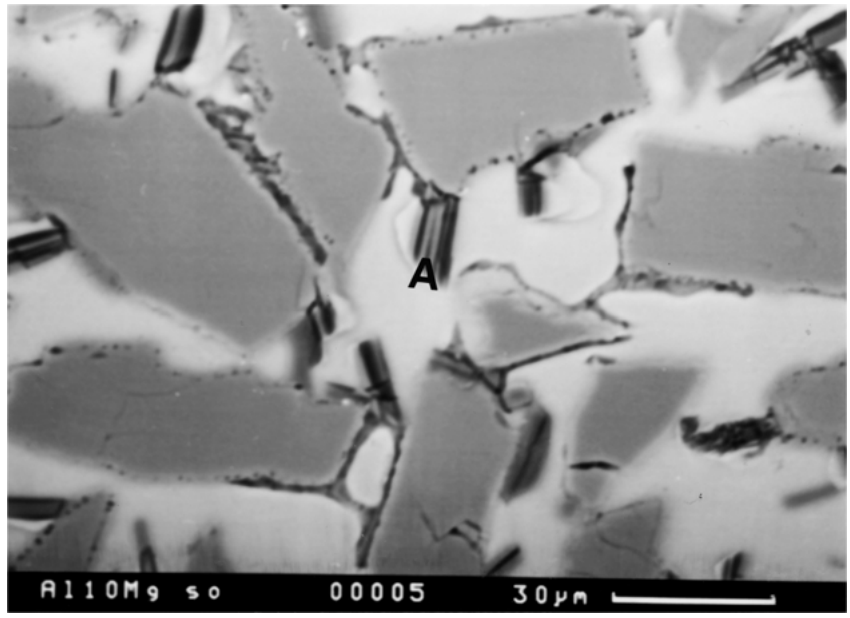

(a)

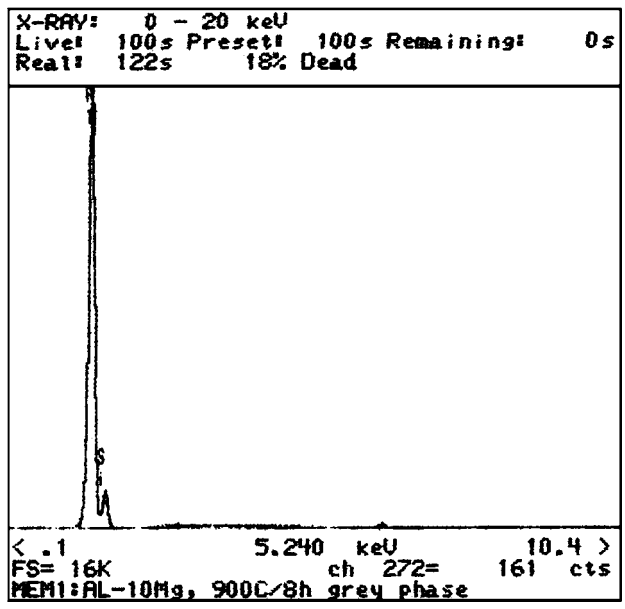

(b)

Figure 6 (a) SEM micrographs of Al-10Mg alloy/SiC MMCs after pressureless infiltration at 900°C for 8 hours. (b) EDS of the A phase.

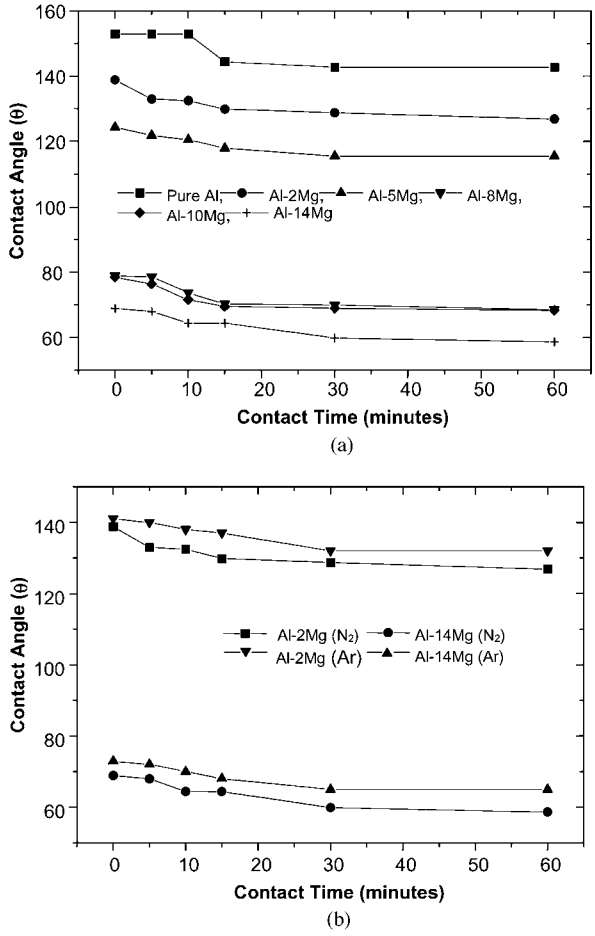

Figure 8 Graphs showing contact angle (θ) Vs holding time (minutes) for pure Al and Al-Mg alloys on SiC substrate at 900°C ± 3°C. (a) under N_2, (b) N_2 and Ar atmospheres.

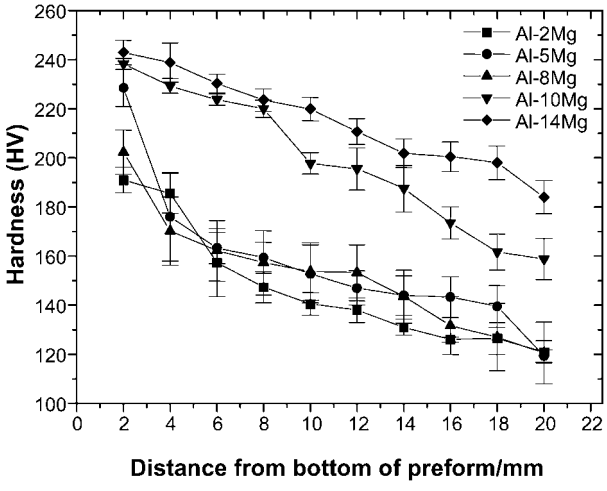

Figure 9 Graphs showing hardness (HV) vs Distance from bottom to the top in Al-Mg alloys/SiC MMCs, after pressureless infiltration at 900°C for 8 hours, under N_2.

in molten Al [24, 25] and reacts as follows :

$$4Al(l) + 3SiC(s) \Leftrightarrow Al_4C_3(s) + 3Si(s) \qquad (2)$$

The Si that is released by this reaction can then react with the Mg to form Mg_2Si.

The aluminium carbide growth from SiC/Al interface has a twinned morphology as seen in Fig. 6. The

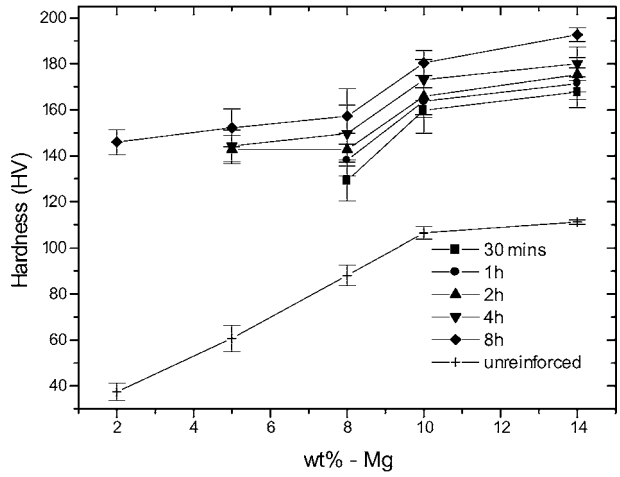

Figure 10 Average hardness (HV) as a function of wt%-Mg in Al-Mg alloys/SiC MMCs after pressureless infiltration at 900°C under N_2.

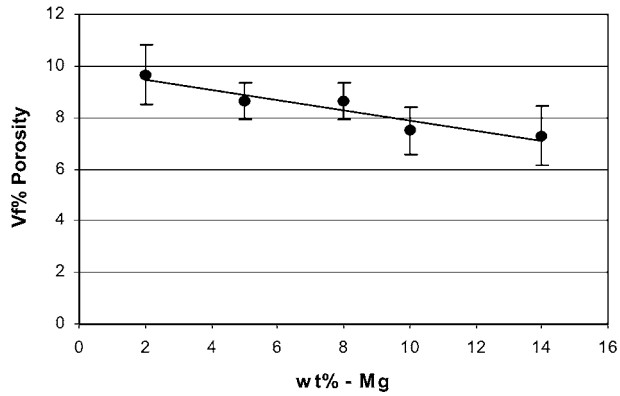

Figure 11 The average porosity (Vf%) as a function of Mg in the Al-Mg alloys/SiC MMC systems after pressureless infiltration at 900°C for 8 hours.

peak height ratio Al_4C_3/SiC indicated that Al_4C_3 increases with increasing infiltration time (Fig. 7), which is in agreement with Lloyd [26] and Lee *et al*. [27] who reported that the amount of Al_4C_3 product on the SiC surface increased with increasing infiltration temperature and time.

The presence of porosity is, to a certain extent, inevitable in infiltration products. Clearly it may arise from entrapped gases, poorly wet regions, shrinkage on solidification and differential shrinkage arising from the different thermal expansion coefficients of the matrix metal and the ceramic reinforcement. In the current work, it was found that there were limited variations in the amounts of porosity produced with different Mg content but that in general the average volume fraction of porosity was reduced with increasing Mg content (see Fig. 11). Given that the wetting characteristics of the Al increased with Mg content it is entirely reasonable that there should be some reduction in the porosity with increasing Mg content. However, it is also noticeable in the current work that there are significant variations in the volume fraction of porosity from the top to the bottom of the specimens produced with porosity levels decreasing from values in the range of 12–16% at the top of the samples down to approximately 2% at the bottom of them for the SiC reinforced systems. In addition, the volume fraction of Al matrix varied from

approximately 70% at the top of composites down to approximately 40% at the bottom of the composites. From these results it can be deduced that the amount of SiC must also vary with position in these composites. The amount of SiC generally increases as one moves from the top to the bottom of the samples. These results imply that infiltration is either tending not to occur, and instead the reinforcing particles are being displaced by the advancing front of molten metal, or that the reinforcing particles are tending to sink in the Al melt after infiltration. The latter situation is thought to be the more likely.

Given that the products have a non-uniform phase distribution it is only to be expected that the hardness distribution within the composites is also non-uniform. The hardness varied with position within the specimen, being greatest near the specimen edges and towards the base of the specimens where the SiC concentration was greatest. Overall the hardness at any particular point was observed to increase with increasing Mg content i.e, as shown in Fig. 9 and summarised in terms of average hardness in Fig. 10. This is to be expected as Al alloys containing these elements are harder than pure Al. In general, increasing infiltration time also led to an increase in the hardness at any particular point.

5. Conclusions

- Wetting contact angles were obtained after 1 hour with the addition of 8 wt%-Mg or higher for Al on SiC under a nitrogen atmosphere. If there was less than 8 wt%-Mg present the contact angle was still greater than 90° after 1 hour. However the infiltration results suggest that the contact angle decreases below 90° even for low Mg contents for times longer than 1 hour.
- There is no indication that infiltration occurs via nitride production. It seems likely that the nitrogen atmosphere is mainly necessary to prevent oxidation and that other inert atmospheres can be used.
- During infiltration SiC particles may react with the Al to give Al_4C_3. The extent of this reaction increases with increasing infiltration time and Mg content. The Si released by this reaction can then react with Mg to form Mg_2Si.
- The composites produced by pressureless infiltration are non-uniform with Al decreasing and the reinforcing phase increasing towards the base of the composites. It is suggested that the microstructural heterogeneities arise in part from differences in density between the molten Al and the reinforcing phase.

Acknowledgements

We wish to thank A Harvey and D Braine for preparing the alloys used in this work. This work was undertaken whilst one of us (AZ) was in receipt of a scholarship from the Indonesian Government Engineering Education Development Project.

References

1. S. RAY, *J Mater. Sci.* **28** (1993) 5397.
2. G. P. MARTIN, D. L. OLSEN and G. R. EDWARDS, *Metal Trans. B* **19** (1988) 95.
3. M. K. AGHAJANIAN, J. T. BURKE, D. R. WHITE and A. S. NAGELBERG, *SAMPE Q.* **20** (1989) 43.
4. M. K. AGHAJANIAN, M. A. ROCAZELLA, J. T. BURKE and S. D. KECK, *J. Mater. Sci.* **26** (1991) 447.
5. A. MORTENSEN and J. A. CORNIE, *Metal Trans. A* **18** (1987) 1160.
6. T. W. CLYNE and M. G. BADER, Fifth International Conference on Composites Materials: ICCM.V. San Diego, CA (1985) p. 755.
7. X. F. YANG and X. M. XI, *J. Mater. Sci.* **30** (1995) 5099.
8. J. W. MCCOY, C. JONES and F. E. WARNER, *SAMPE Q.* **19**(2) (1988) 37.
9. G. H. SCHIROKY, D. V. MILLER, M. K. AGHAJANIAN and A. S. FAREED, *Key Engineering Materials* **127–131** (1997) 141.
10. T. WATARI, K. MORI, T. TORIKAI and O. MATSUDA, *J. Amer. Ceram. Soc* **77** (1997) 2599.
11. D. J. LLOYD, H. LAGACE, A. MCLEOD and P. L. MORRIS, *Mater. Sci. Eng.* **A107** (1989) 73.
12. D. J. LLOYD and I. JIN, *Metal Trans. A* **19A**(1988) 3107.
13. J. C. VIALA, P. FORTIER and J. BOUIX, *J. Mater. Sci.* **25** (1990) 1842.
14. Y. Y. CHEN and D. D. L. CHUNG, *ibid.* **31** (1986) 407.
15. T. CHOH, M. KOBASHI, H. NAKATA and H. KANEDA, *Mat. Sci. Forum* **217–222** (1996) 353.
16. K. B. LEE and H. KWON, *Scripta Mater* **36** (1997) 847.
17. A. J. MCEVOY, R. H. WILLIAMS and I. G. HIGGINBOTHAM, *J. Mater. Sci.* **11** (1976) 297.
18. A. BARDAL, *Mater. Sci. & Eng.* **A159** (1992) 119.
19. A. PAPWORTH and P. FOX, *Mater. Sci. Technol.* **13** (1997) 912.
20. X. GU and R. J. HAND, *J. Europ. Ceram. Soc.* **16** (1996) 929.
21. A. S. NAGELBERG, *Solid State Ionics* **32/33** (1988) 783.
22. X. GU and R. J. HAND, *J. Europ. Ceram. Soc.* **15** (1995) 823.
23. A. ZULFIA and R. J. HAND, *Mater. Sci. Technol.* **16** (2000) 867.
24. R. WARREN and C. H. ANDERSSON, *Composites* **15** (1984) 101.
25. T. ISEKI, T. KAMEDA and T. MARUYAMA, *J. Mater. Sci.* **19** (1984) 1692.
26. D. J. LLOYD, *Composites Sci. Technol.* **35** (1989) 159.
27. K. B. LEE, Y. S. KIM and H. KWON, *Metal Trans. A* **29** (1998) 3087.

Received 1 February
and accepted 18 October 2001